The United Nations University

GEOTHERMAL TRAINING PROGRAMME
Orkustofnun, Grensasvegur 9,
IS-108 Reykjavik, Iceland

Reports 1994
Number 8

INTERPRETATION AND SIMULATION OF THE HAMAR GEOTHERMAL FIELD, N-ICELAND

Li Cheng
Department of Earth Sciences,
Nanjing University, Nanjing, 210008,
P.R. CHINA

ABSTRACT

The Hamar reservoir is one of many low-temperature geothermal fields in Northern Iceland. Since 1966 eleven wells have been drilled in the field but at present only well 11 is producing. About 44 temperature logs were taken from 1966, and water level changes and production rates have been recorded since 1975. Well tests were performed in 1988. On the basis of these data, the thermal characteristics of the reservoir were analyzed, and the main aquifers or feedzones identified. The hot water recharge comes from the south. After most of the wells were cased and/or cemented in 1990, the temperature in the reservoir has remained constant. The physical behaviour of the reservoir was simulated using a lumped parameter model. Water level changes with various production rates for the next 20 years are given. Analyses of well test data from the reservoir were made using Theis solution and Horner methods. The same results were obtained using both methods. The reservoir has a transmissivity of about 5.5×10^{-7} m^3/Pa s, coefficient of storativity ($c_t h$) of about 7.5×10^{-8} m/Pa and a calculated reservoir thickness (h) of about 1500 m.

1. INTRODUCTION

In exploiting a geothermal area, it is very important to measure the pressure and temperature in the reservoir before production and during exploitation. Such data can be used as an aid in further exploration, to help with the management of the field and in simulations of the geothermal field in order to make predictions for further exploitation.

Temperature logging is a powerful method to obtain information about the thermal state of a reservoir and to calculate heat flux as well as geothermal gradient. Analysis of temperature logs can also give information about the hydrodynamics of flow within the geothermal field. Combined with other information, feedzones or aquifers can be inferred from temperature logs. Pressure transient testing is a method to estimate some physical properties of the reservoir that can be used in simulating the behaviour of the field.

The purpose of modelling the behaviour of geothermal reservoirs under a variety of exploitation schemes is to obtain knowledge of the physical processes needed for further exploitation, control and management. The Hamar reservoir is a low-temperature geothermal field in N-Iceland. It has a 20-year exploitation history. In this report, the author begins by analysing temperature logs and well test data, then uses a lumped parameter model to fit the calculated pressure changes to the 12 years of observed water level data. From these, a prediction of the water level changes for the next 20 years is made for various production rates.

2. THE HAMAR GEOTHERMAL FIELD

2.1 Location

Hamar in N-Iceland (65°57'N, 18°32'W) is a small geothermal field utilized by a district heating service that serves Dalvík, a small town of 1400 inhabitants, located by the seashore. Hamar is approximately 5 km south of the town in the slopes of a hill, 60 m above sea level. Since 1966, eleven wells have been drilled in the field (Figure 1). Of these, only four wells have produced. These are wells 2, 9, 10 and 11. Well 2 was in production from 1970-1975; well 9 from 1975 to 1977; well 10 from 1977-1988; and well 11 from 1988 to present. The last well drilled is the deepest at 860 m. The production wells have feedzones between 500 and 800 m depths (Axelsson, 1989), with water temperature of 64°C. During drilling free-flow appeared from wells 1, 3, 5, and 8 in which wellhead pressures were estimated to be 1-1.5 bars. During April-September 1990 wells 1, 2, and 6 were filled with cement; wells 3, 4, and 5 were cased and cemented to the bottom; and wells 7 and 9 were cased with a perforated casing at the feedzones, which means they show true water level. Table 1 shows the characteristics of the wells.

TABLE 1: Main characteristics of the wells at Hamar

Well no.	Drilling completed	Depth (m)	Casing		Production period
			Width (")	Length (m)	
1	Dec. 1966	101	4*	0-2.4	never
2	Jan. 1969	300	8*	0-38.0	1970-1975
3	Apr. 1969	504	10; 8**	0-5.3; 5.3-39.4	never
4	Jun. 1969	303	8**	0-28.0	never
5	Feb. 1971	587	7**	0-60.0	never
6	Mar. 1971	373	12*	0-3.0	never
7	Jul. 1971	302	8***	0-78.0	never
8	Jul.1974	108	4	0-8.8	never
9	Sept. 1975	253	10***	0-119.0	1975-1977
10	Sept. 1977	838	10 3/4; 9 5/8	0-122.2; 122.2-174.6	1977-1988
11	Aug. 1987	860	11 3/4	0-253.6	1988-now

* Filled with cement; ** Cased and cemented to the bottom;
*** Cased with a perforated casing at the feedzones.

2.2 Geology and geophysics

The Hamar geothermal field is located in a mountain slope about 65 km from the neovolcanic zone in N-Iceland in a 6-10 m.y. old formation. The main layers consist of porphyritic basalt and tholeiitic basalt. There are some thin scoriae and sediments between the basaltic layers. The layers generally dip 3-4° toward southwest (Figure 2). An axis of an anticline can be seen some 4 km to the northeast of the geothermal field. The basaltic lava pile is intersected by numerous near vertical dykes and normal faults which probably are a part of a fissure swarm belonging to an ancient and extinct central volcano 10-20 km away from Hamar. The regional temperature gradient outside the hydrothermal area is close to 60°C/km, and the heat flow to the surface is about 150 mW/m^2 (Flovenz and Saemundsson, 1993). It reflects the heat conducted through the crust from the underlying mantle. Rybach (1988) estimated the heat generation rate of basalt to be 0.309 $\mu W/m^{-3}$.

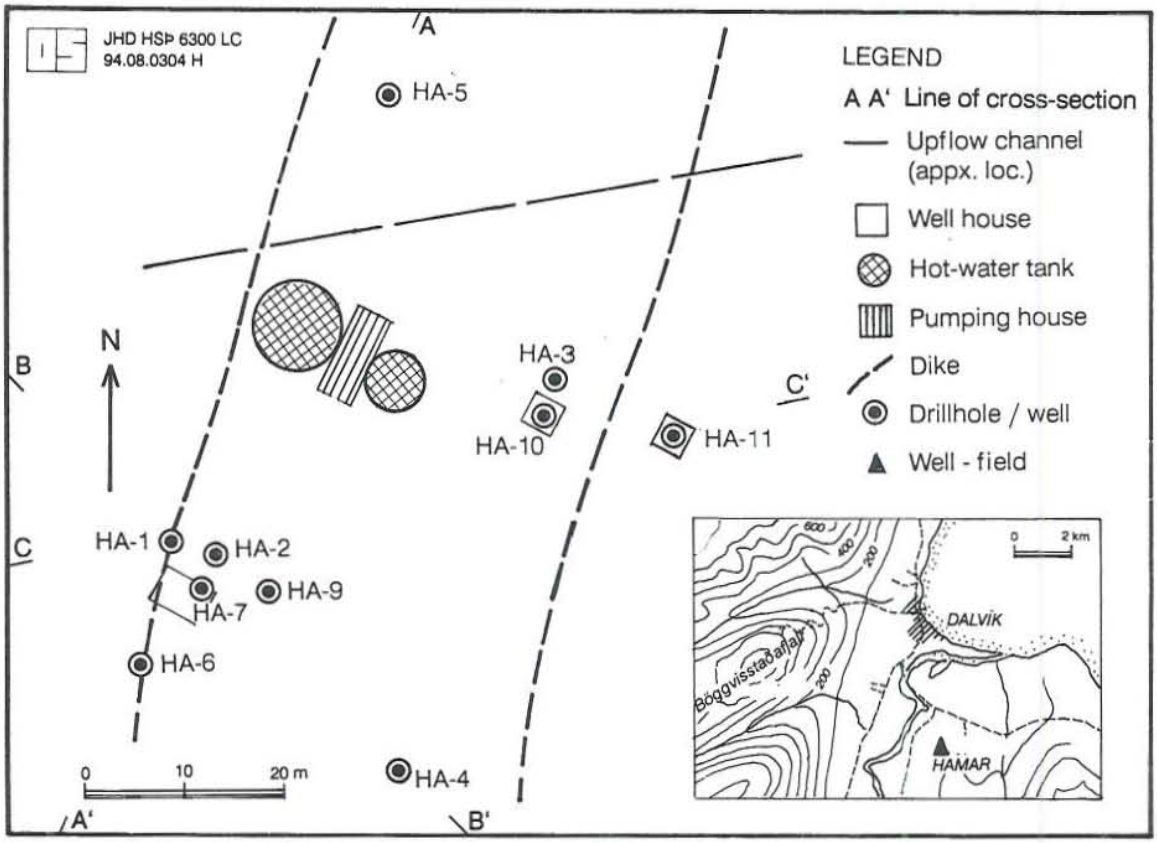

FIGURE 1: Location map of the well-field at the Hamar geothermal field in N-Iceland (modified after Karlsdottir and Axelsson, 1986)

There are indications that most of the present low-temperature geothermal fields in Iceland were formed by crustal movements during the last deglaciation and are therefore about 10,000 years old (Bodvarsson, 1982). It has been proposed that tectonic movements, that followed the deglaciation, formed macroscopic fractures in which convection started and formed geothermal systems (Flovenz and Saemundsson, 1993). Once the convection is initiated it is a self-renewable process, contraction in the deepest part of a fracture due to heat-mining will extend the fracture to greater depth and the convecting liquid comes continuously in contact with new hot rock (Axelsson, 1989).

3. ANALYSIS AND INTERPRETATION OF THE TEMPERATURE DISTRIBUTION

3.1 Analysis of temperature logs and feedzones

Temperature logs are a set of temperature values recorded at different depths down a borehole, which can give information about the characteristics of the formation penetrated by the borehole. In the Hamar geothermal field, many temperature logs have been taken during drilling and production. Information about the temperature logs from the eleven wells at the Hamar field is summarized in Table 2, and they are shown in Figures 3 and 4.

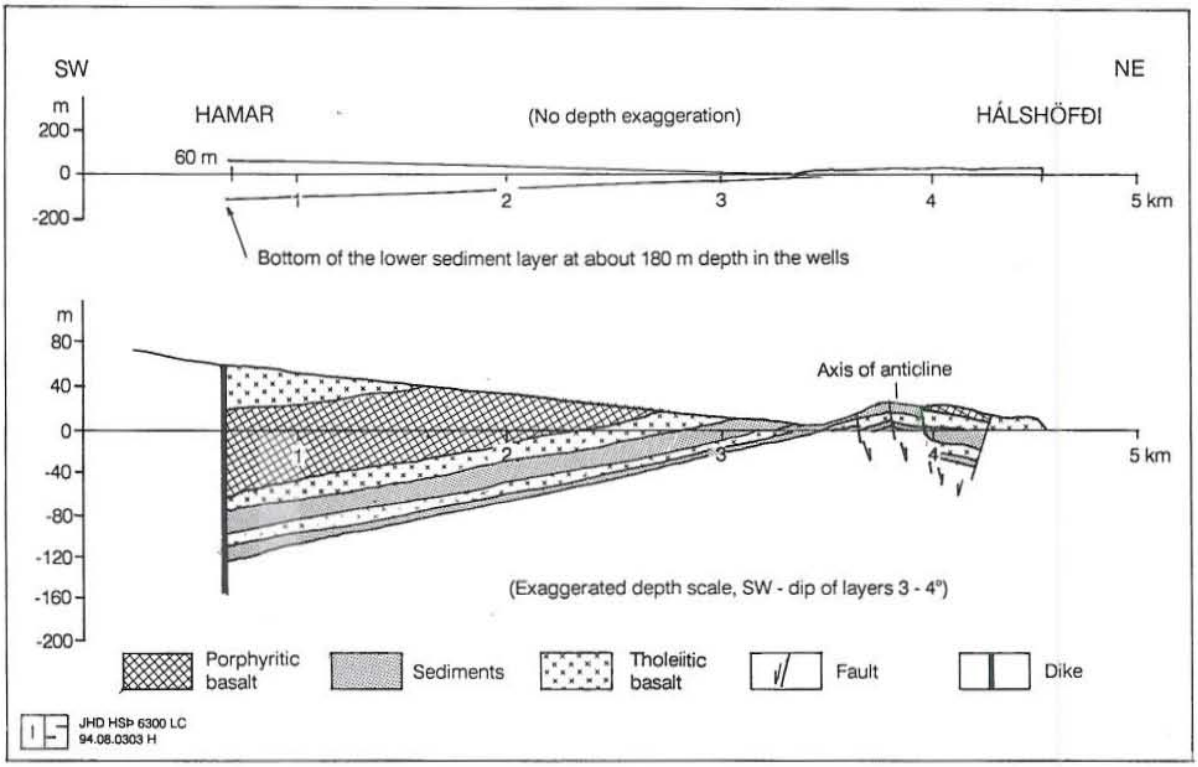

FIGURE 2: Geological cross-section from Hamar to Halshofdi (modified after Saemundsson, 1970)

Well 1: The first well at Hamar, 101 m deep, was completed in 1966. The well is situated near the western dyke. Altogether there are four temperature logs from the well (Figure 3). The first temperature log was taken during drilling when there was a free-flow from the well. The second temperature log was made 9 months later. The two temperature logs which reached only 30 m are very similar, and show an up-flow of 48°C hot water coming from 30 m depth or below. Another two temperature logs were taken in 1971 and 1985 after well 2 had been producing. In these logs the free-flow had disappeared but a downflow of cold water of about 15°C had started. No feedzone can be identified from the temperature logs because of the flow in the well, but at least one is located below 30 m..

Well 2: The well was drilled to 300 m in 1969. The first temperature log was taken in 1985, and the second in 1990. The well was the production well between 1970 and 1975 (Figure 3). The temperature changes between the two temperature logs are mostly above 60 m depth where the later one is colder by about 6°C from 30 to 50 m depth. In the second log a downflow of 23°C water can been seen between the feedzones at 40 and 60 m. Three feedzones can be seen at 120, 135 and 150 m depth

Well 3: The well was completed to 504 m depth in 1969 and the first temperature log was taken during drilling (Figure 3). A free-flow appeared from 150 m depth and two feedzones at 160 and 200 m can be identified in the log. When well 2 started production in 1970 the free-flow from the well stopped. The second temperature log was taken in 1971 and the borehole temperature seemed to increase by about 3-6°C. After the well was cased to the bottom in 1990, another temperature log was taken in 1991. Because of the casing this temperature log can be considered as the formation temperature. A horizontal flow at about 160 m depth close to the well can be seen in the log. Compared to the previous temperature logs, the temperature profiles are similar above 50 m, and 3-6°C cooling can be seen below this depth. The last log was taken in 1994; it is identical to the one from 1991. This shows that no cooling has taken place since 1991.

TABLE 2: Temperature logging and water level at the Hamar geothermal field

Well No.	Drilling dates from...to...	Temperature logging dates			Water level (m)
		during drilling	before prod.	after prod.	
1	Nov. 1966	01.12.1966			free-flow
	Dec. 1966		02.09.1967		2.0*
			09.05.1971		2.25
			17.07.1985		22.0
2***	Dec. 1968			17.07.1985	22.0
	Jan. 1969			15.06.1990	16.0
3**	Feb. 1969	01.04.1969			free-flow
	Apr. 1969		10.02.1971		7.7
			15.06.1990		12.5
			30.08.1991		10.0*
			25.08.1994		5.5
4**	Apr. 1969		10.02.1971		50.0*
	Jun. 1969		14.08.1972		50.0*
			16.07.1985		10.0*
			15.06.1990		20.0*
			26.10.1991		7.0*
			24.08.1994		
5**	Nov. 1970	17.02.1971			free-flow
	Feb. 1971		17.07.1985		20.0
			07.08.1991		1.6
			24.08.1994		5.15
6***	Feb. 1971		14.08.1972		50.0*
	Mar. 1971		18.07.1974		20.0*
			12.10.1974		58.0*
			16.07.1985		9.0*
7**	Jun. 1971		14.08.1972		50.0*
	Jul. 1971		17.07.1974		20.0*
			15.06.1990		15.5*
			30.08.1991		12.0
			24.08.1994		11.8
8	May. 1974	18.07.1974			free-flow
	Jul. 1974		31.10.1974		5.0*
			11.10.1975		5.0
			17.07.1985		0.0*
			24.08.1994		0.0
9**	Jul. 1975	21.08.1975			21.0
	Sept. 1975			30.08.1991	12.5
				24.08.1994	11.6
10	Aug. 1977			25.05.1988	20.0*
	Sept. 1977				
11	Jul. 1987		22.07.1987		20.0*
	Aug. 1987		09.08.1987		50.0*
			12.08.1987		40.0*
			12.08.1987		240.0*
				25.05.1988	17.0

* The depth of temperature logging starting point;
** Cased during April-September 1990;
*** Filled with cement during April-September 1990.

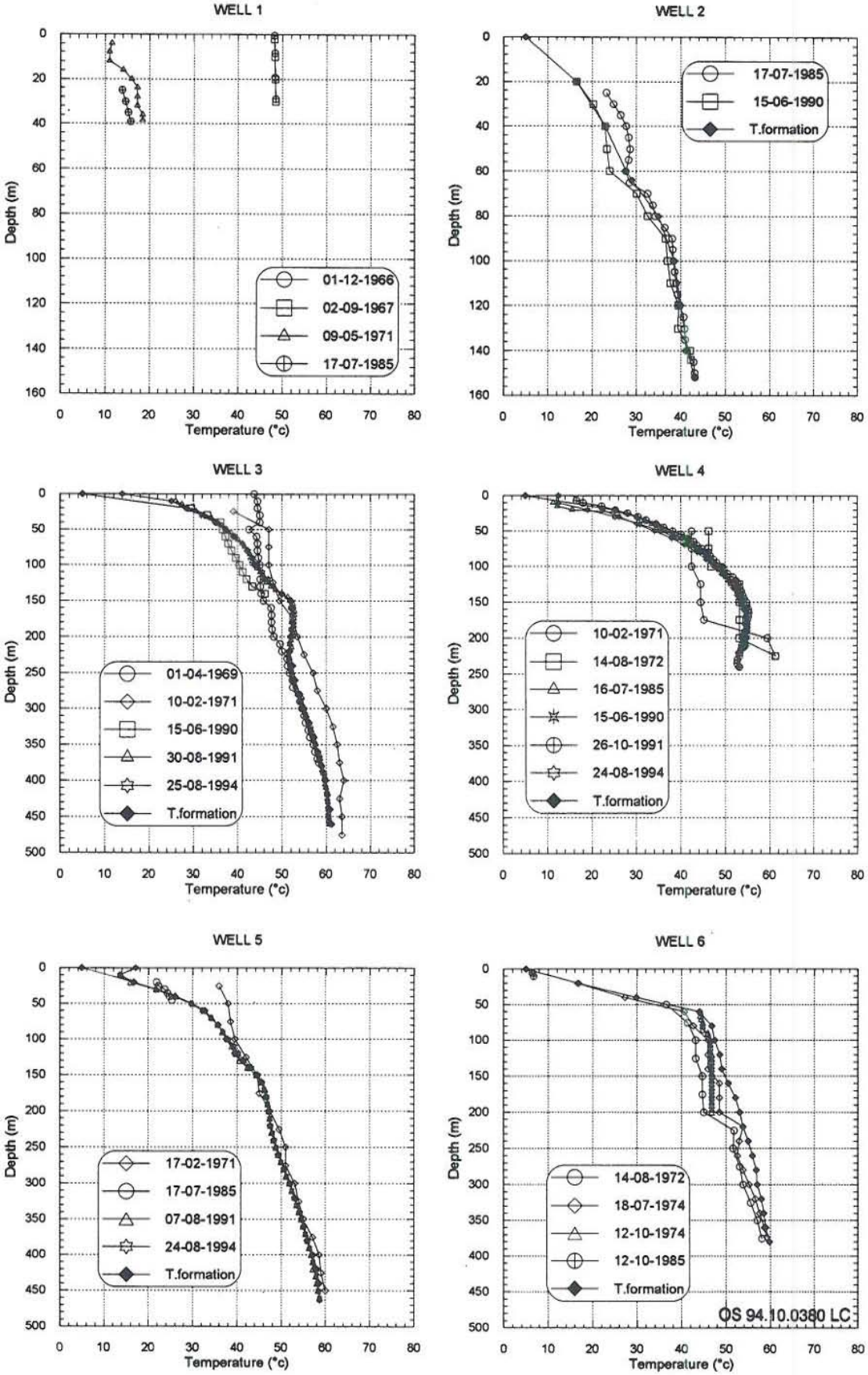

FIGURE 3: Temperature logs in wells 1-6 at Hamar

Well 4: The well is 303 m deep. Since drilling was finished in 1969, six temperature logs have been taken (Figure 3). The first temperature log (in 1971) shows a down-flow of 43°C from 50 to 175 m depth. The hottest measured temperature was 62°C at 220 m which is probably the formation temperature before production. When the well was measured in 1972, there was a flow from 50 m (or above) down to 100-125 m, where some hotter water entered the well and flowed down to 175-200 m depth. So, there are at least three feedzones that can be identified in the well (≤50, 100-125, and 175-200 m). The measurement from 1985 shows a general cooling of up to 10°C near the bottom. A casing was cemented in the well in 1991, after which the temperature seems to have increased by 2-3°C. The last log from 1994 is very similar to that from 1991 which indicates stable conditions in the well.

Well 5: The well was drilled to 587 m depth in 1971. Four temperature logs were taken (Figure 3). The first log was taken 7 days after drilling in 1971, and shows a down-flow of 52°C water from 250 to 275 m. The second log was only taken from 20 to 45 m in 1985. Compared with the first log, cooling of about 10°C between 20 to 45 m can be seen. The third temperature log in 1991 was done after a casing was cemented in the well, but shows 2-3°C cooling from the first one. A fourth log was performed in 1994 which shows that the well is now in a stable condition and that the curve can be considered to be the formation temperature.

Well 6: The well was drilled to 373 m depth in 1971. Four temperature logs have been taken (Figure 3), the first in 1972. A down-flow appeared from 100 to 200 m, and another down-flow can be seen between 225 and 250 m. Four feedzones can be identified in the well (100, 200, 225, and 250 m). A horizontal flow can be seen at 230 m depth. The second log was taken in 1974 where two zones of down-flow were observed, one at 100-140 m and another at 160-200 m with temperatures of 46 and 48°C, respectively. A horizontal flow can be seen at the same depth as in the first log. The second log shows a general warming of about 2-4°C. Four feedzones can be identified: at 100, 140, 160, and 200 m. The third log was taken in 1974. The two down-flow zones can be seen very clearly, one of which is 45°C from 60 to 85 m and the other one 47°C from 90 to 200 m. Four feedzones can also be seen; at 60, 86, 90, and 200 m. The last log was taken in 1985 down to 20 m depth.

Well 7: The well was drilled to 302 m depth in 1971. The first temperature log was taken one year after drilling (Figure 4). At about 130 m depth a horizontal flow of hot water came close to the well at that time. The second log is similar but 2°C warmer above 200 m depth. The next two temperature logs from 1990 and 1991 show two feedzones at 120 and 200 m. The 120 m feedzone corresponds to the horizontal flow seen in the 1972 and 1974 logs. A cooling in the well is clear above 200 m, with maximum change of 25°C at 50 m compared to the first two temperature logs. Almost no temperature changes occur below 200 m in the five temperature logs.

Well 8: The well is 108 m deep and was finished in 1974. The location of the well is outside Figure 1, about 177 m north of well 5. During drilling when the first temperature log was taken, there was a free-flow of 8°C at the well head (Figure 4). The other three temperature logs were taken in 1974, 1975, and 1985. No obvious flow occurs in the well. The last log was taken in 1994, identical to the previous logs. The logs can be considered as the formation temperature and show a constant temperature gradient of about 150°C/km.

Well 9: The well was drilled in 1975 to 253 m depth. The well had an interval of production from 1975 to 1977. The first temperature log was measured during drilling in which three feedzones were seen at 25, 40-50, and 100 m depths (Figure 4). The second temperature log was taken in 1991 after the well was cased down to the bottom. At 230 m a low-temperature anomaly was found where there is a horizontal flow. The last log was taken in 1994. The temperature log curve is very similar to the log from 1991 and can be considered as the formation temperature.

Well 10: The well is 838 m deep and was drilled in 1977. The well was the Hamar producer 1977-1988. Only one temperature log was recorded (Figure 4). Nothing can be inferred about the formation temperature, apart from being about or higher than 65°C at the bottom.

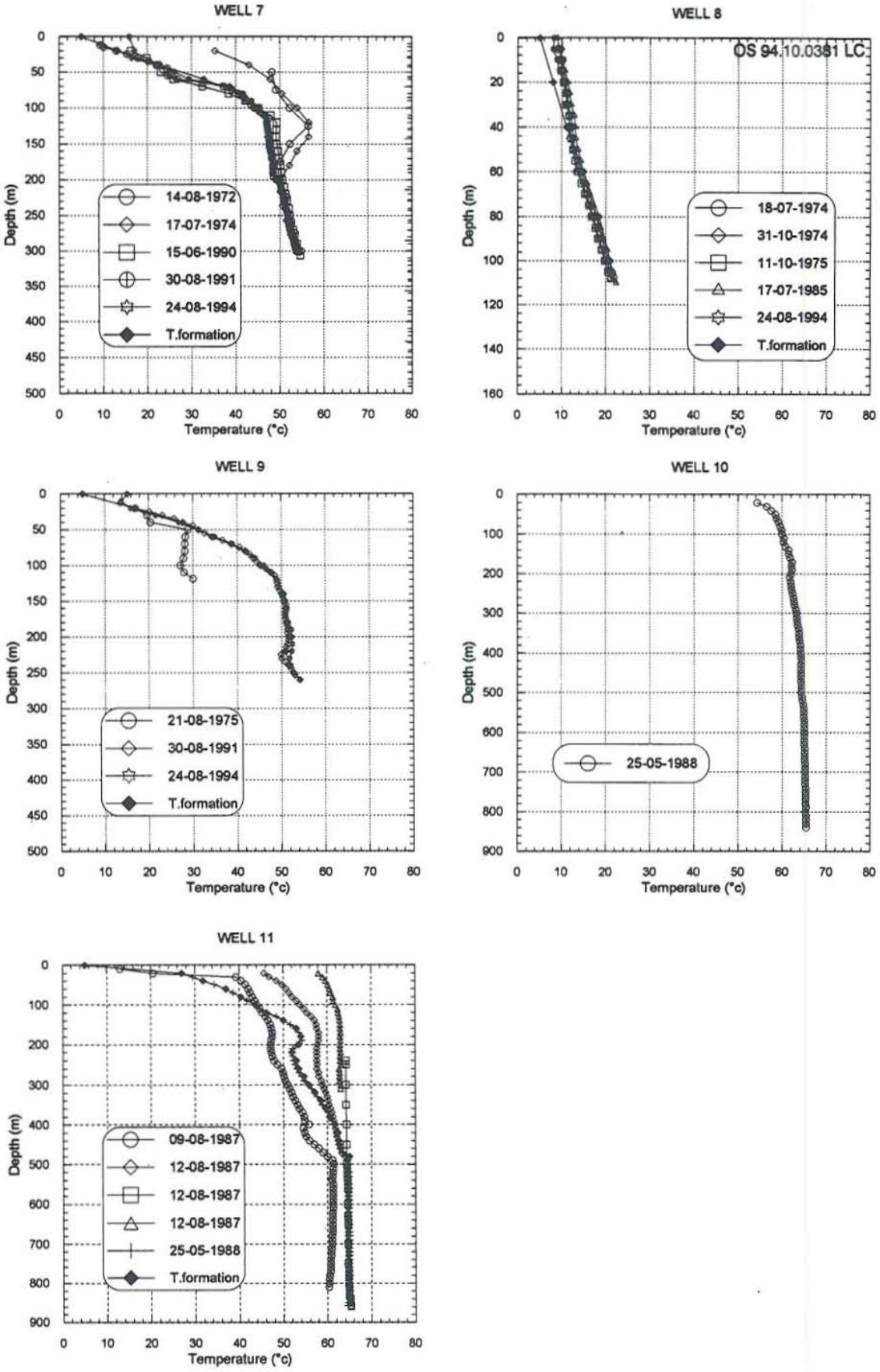

FIGURE 4: Temperature logs in wells 7-11 at Hamar

Well 11: The well was drilled in 1987, and is the deepest in the area, 860 m. Since 1988 when production from well 10 stopped, well 11 has been the only production well at Hamar. Four temperature logs were measured in the same month in 1987 (Figure 4). The warming from the first log represents temperature recovery after drilling. An up-flow occurred from the bottom. The last temperature log was taken is 1988 which shows a high-temperature anomaly at 180 m depth. Four feedzones can be identified in the well, at the bottom, at 190, 220, and 490 m.

Locating feedzones is one of the main purposes of temperature log analysis. A feedzone is a channel for convecting water or vapour in a geothermal reservoir. In geology, feedzones correspond to fracture belts or the formation that possesses high permeability and porosity. Feedzones can be identified from some geophysical logs. Further research is needed in order to determine the size of a feedzone, including circulation loss and alteration intensity as well as analysing a Neutron-neutron log. Figure 5 represents the main feedzones of the eleven wells at Hamar.

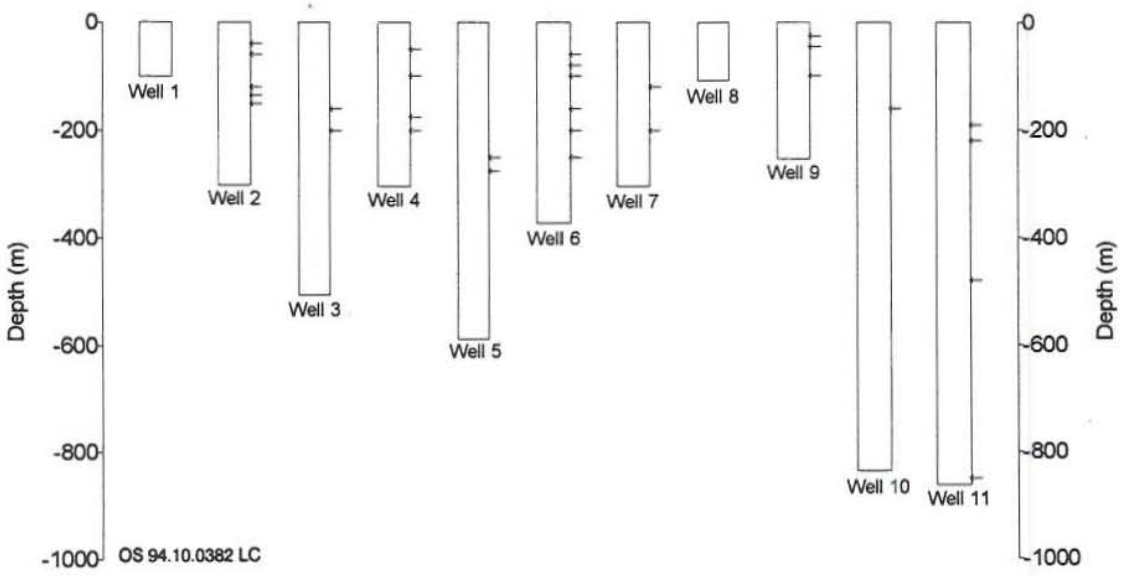

FIGURE 5: Location of feedzones in wells 1-11 at Hamar

3.2 Formation temperatures and temperature profiles

The formation temperature in a well is the true or static temperature in the formation around the well. Generally, the information about the reservoir temperature comes from temperature logs but it is necessary to take several factors into consideration when the true temperature is estimated. These are the circulating drilling fluid, down-flow or up-flow in the well and condition in the well before and during logging. There are some methods that permit the determination of the static formation temperature. In this section several principles are used to get the formation temperature from temperature logs:

1) The maximum recorded bottomhole temperature (BHT);
2) The temperature log after casing or cementing;
3) Analysing and deleting the disturbance from up- or down-flows in the well.

According to the above all temperature logs have been analysed one by one, and the formation temperature at each well has been estimated (Figures 6). The change in the formation temperature with depth is faster at shallow depths. The changes in temperature between two temperature logs is also bigger at shallow depths than at greater depths. This shows that the temperature gradient is higher at shallow depths, i.e. above 150-200 m.

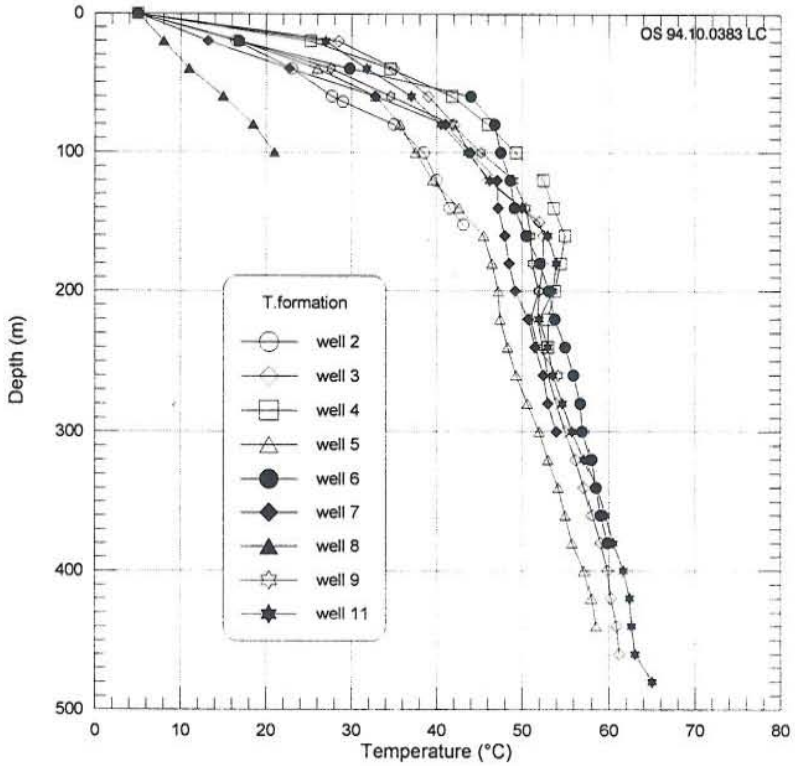

FIGURE 6: Formation temperature in the Hamar wells

To get the temperature characteristics in the field, three temperature cross-sections were drawn, the location of which can be seen in Figure 1. These cross-sections are drawn on the basis of the formation temperature analysis. The temperature anomalies give indications of the flow pattern in the area and possible location of faults and dykes (Figures 7, 8 and 9). There is a high-temperature anomaly that indicates up-flow between the two dykes, which were found by a magnetic survey.

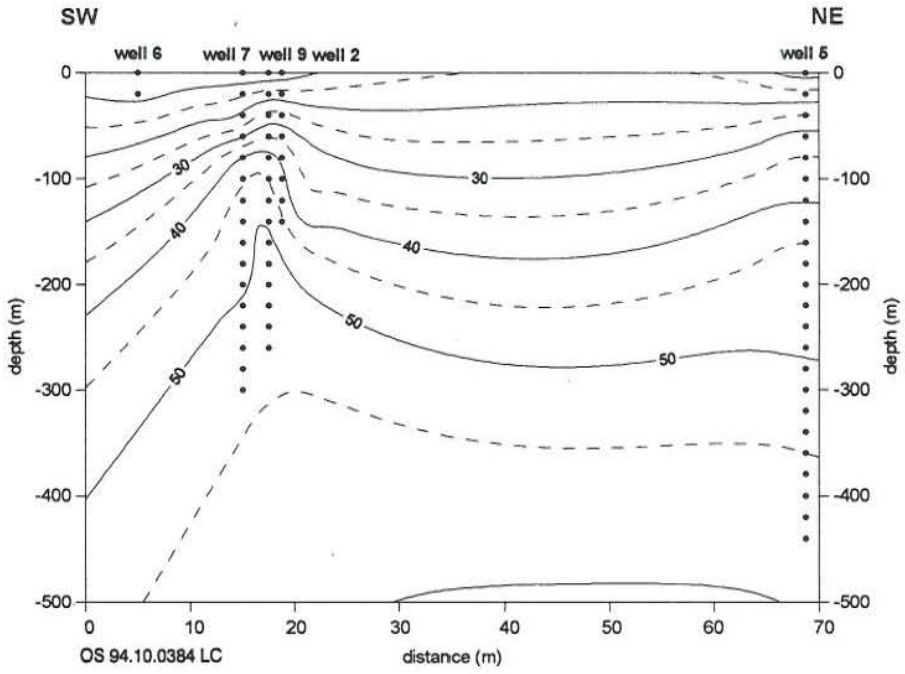

FIGURE 7: Temperature cross-section A-A'

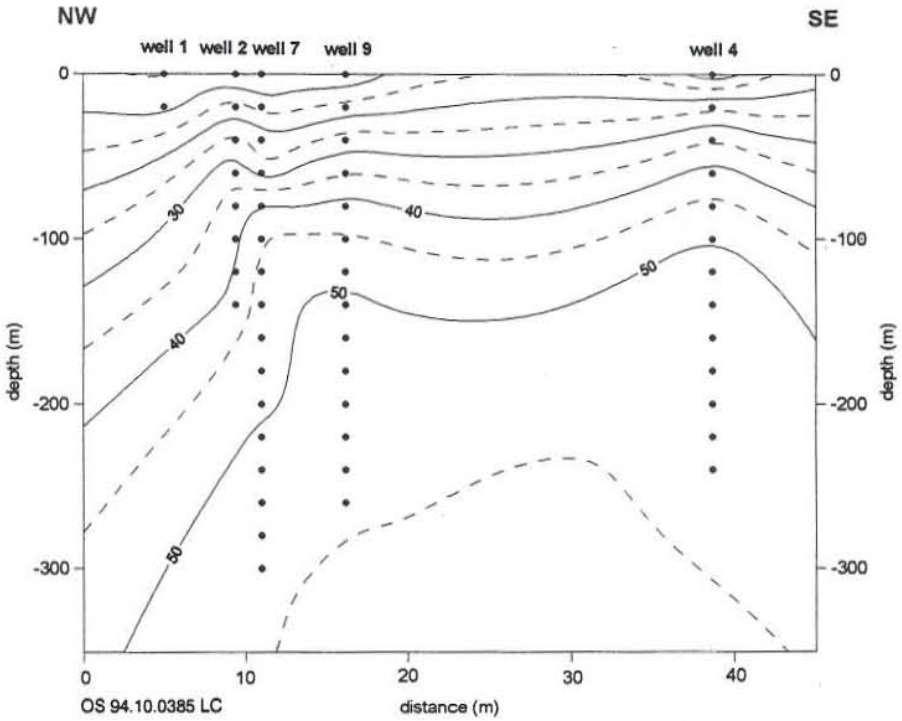

FIGURE 8: Temperature cross-section B-B'

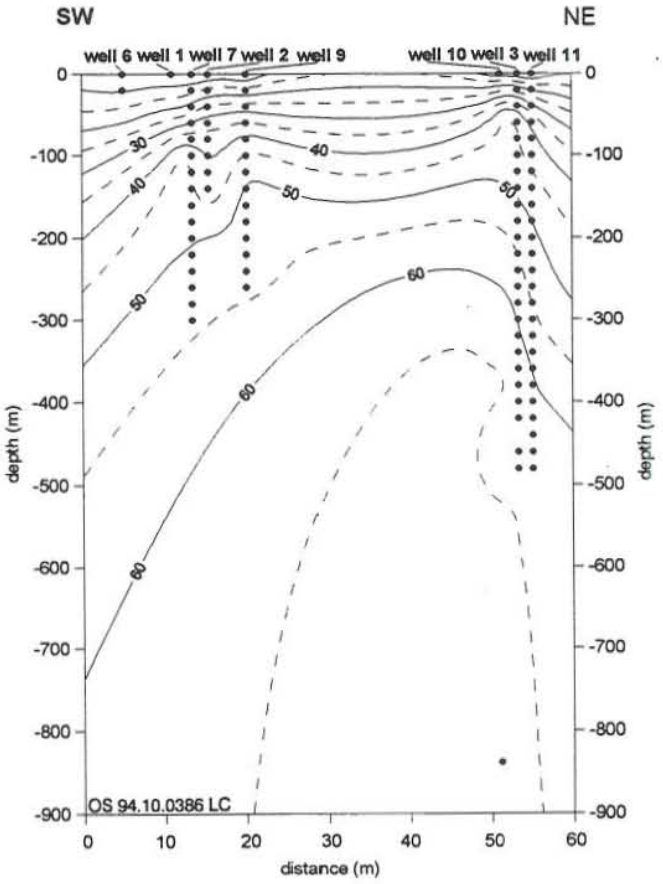

FIGURE 9: Temperature cross-section C-C'

Based on the formation temperature at each well, the temperature distribution was plotted at different depths (Figures 10, 11, 12, 13). At 40 m depth the isotherms illustrate that there is an area of anomalously high-temperature along the eastern dyke. The lowest temperatures are at the western dyke. The strike of the isotherm lines is almost N-S and the isotherm plane slopes to the west. This characteristic disappears at 100 m depth and the isotherms do not show the obvious high or low-temperature areas. At 100 m depth the isotherms strike is now in the E-W direction instead of N-S as above, and the isotherm plane inclines to the north which is considered to be the cooling direction. The isotherms at 200 and 300 m depths are similar, but the tendency is clear that with increasing depth, the slope of the isotherm plane increases.

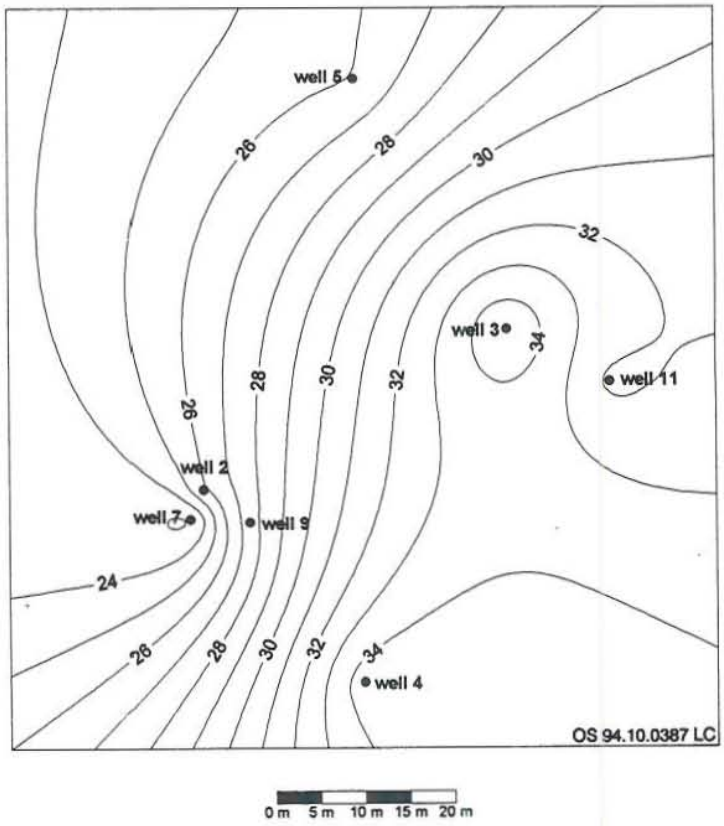

FIGURE 10: Isotherms (°C) in the Hamar field at 40 m depth

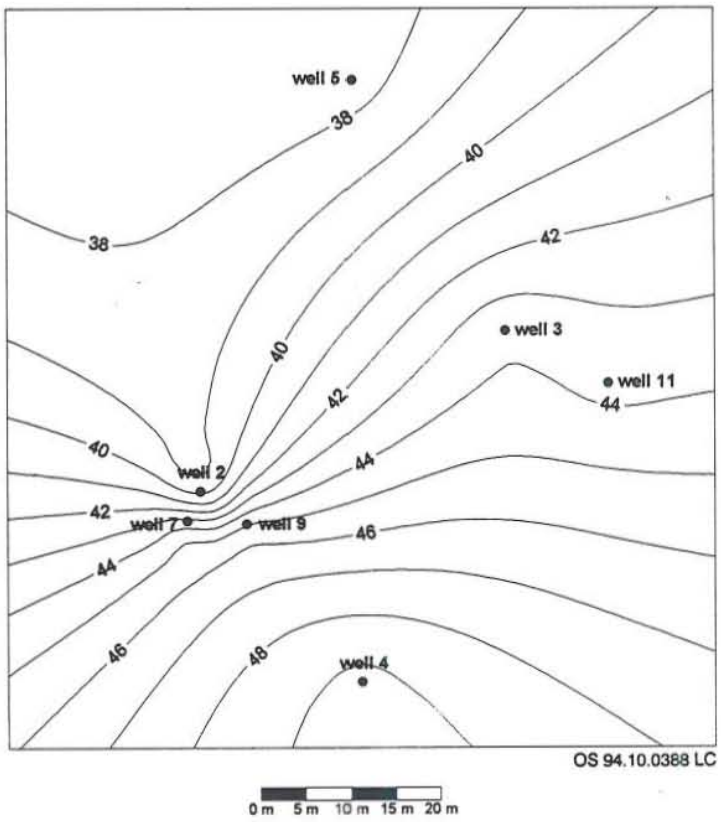

FIGURE 11: Isotherms (°C) in the Hamar field at 100 m depth

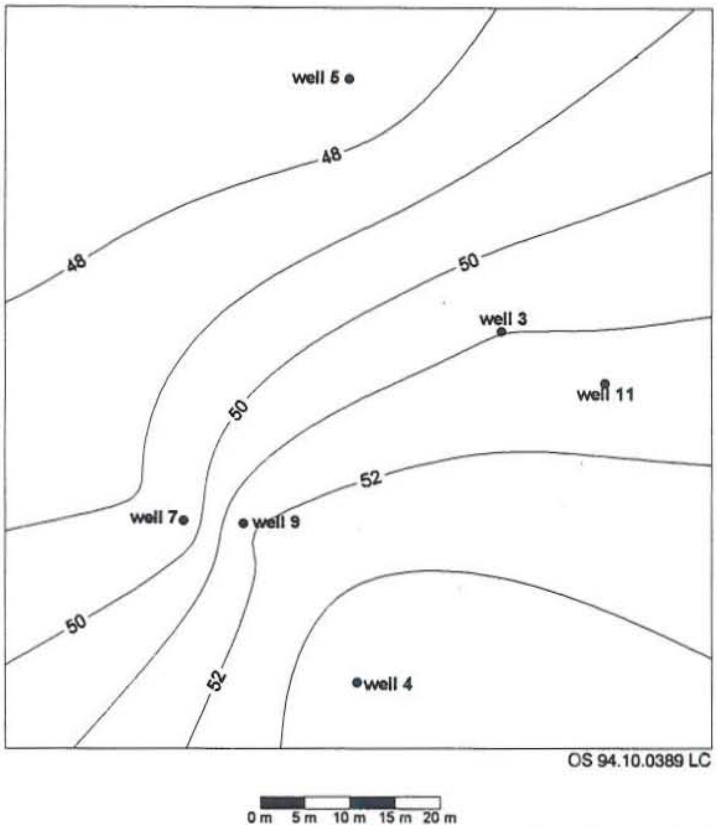

FIGURE 12: Isotherms (°C) in the Hamar field at 200 m depth

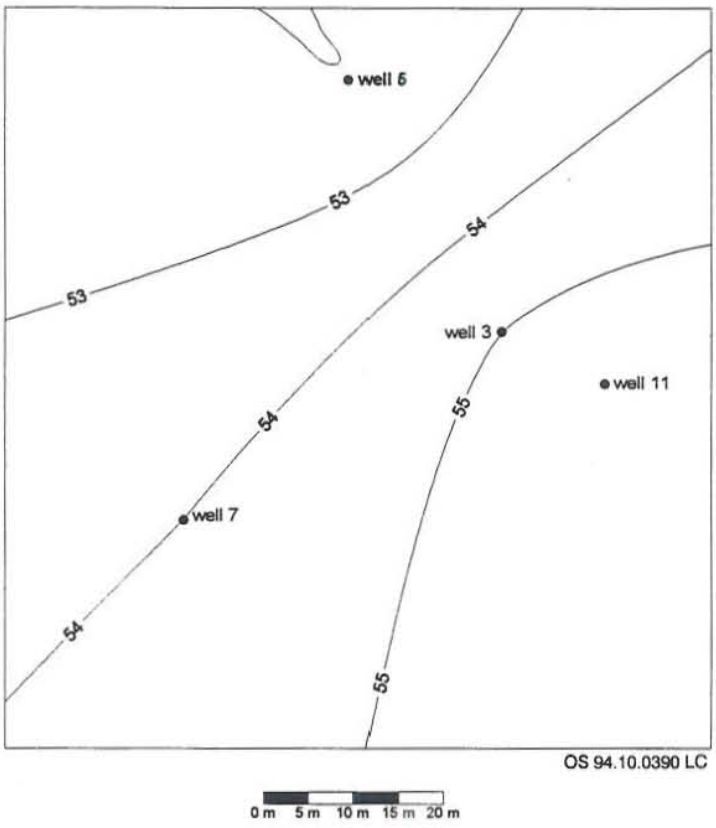

FIGURE 13: Isotherms (°C) in the Hamar field at 300 m depth

4. SIMPLE SIMULATION OF THE HAMAR GEOTHERMAL FIELD

4.1 Theory and methods of calculation

The term reservoir simulation means the process of deducting the physical behaviour of a real reservoir from the performance of a model (Edwards et al., 1982). The primary objective of mathematical modelling of geothermal reservoir is to obtain data that will assist the field developer in his decision-making process. As a tool for resource assessment, it has grown significantly during the last decade.

Simple simulation, such as lumped parameter models, is characterized by one or more parameters representing a combination of primary parameters or regions of the reservoir. Lumped parameter models have been developed for many geothermal reservoirs (Bodvarsson et al., 1986).

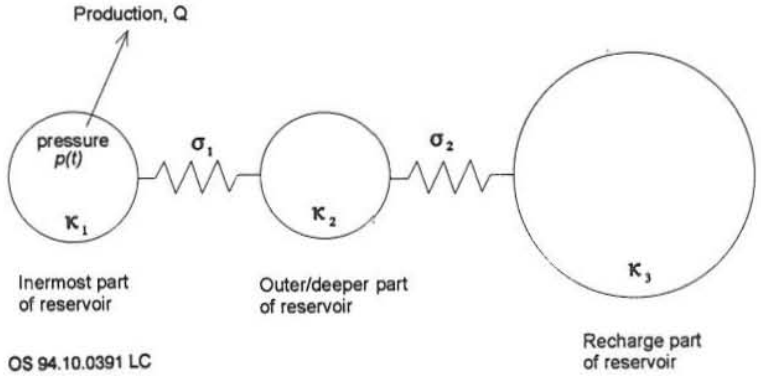

FIGURE 14: General idea of the lumped parameter model (Axelsson, 1989)

Figure 14 shows the principal train of thought. Most lumped parameter models use two or three tanks to represent the entire system. One of the tanks represents the well field, and the others act as recharge parts from depth or outside of the main reservoir. This method tackles the simulation problem as an inverse problem. It automatically fits analytical response functions of lumped models to the observed data by using a non-linear iterative least-squares technique for estimating the model parameters (Axelsson, 1989). Each tank ignores the reservoir shape. This network of tanks is considered to be either open or closed. When the network is open, one of the tanks is connected to a system of constant pressure. When the network is closed, the tanks are not connected to an outside recharge system and the pressure of the system declines as production proceeds.

On the basis of the illustration of the lumped parameter model above, the mathematical model for the system is as follows:

$$\kappa = \frac{m}{p} = Vs = V\rho_w c_t \tag{1}$$

and

$$\sigma = \frac{q}{\Delta p} = \frac{kA}{\nu L} \tag{2}$$

If there are N tanks, the massflow between tank i and tank k is q_{ik}, the resistor between tank i and tank k is σ_{ik} the production from tank i is Q_i, and p_o is equilibrium pressure. Then, the basic equations to describe

massflow and pressure change in the tanks can be expressed as

$$q_{ik} = \sigma_{ik}(p_k - p_i) \tag{3}$$

$$\kappa_i \frac{\partial p_i}{\partial t} = \sum_{k=1}^{n} q_{ik} - \sigma_i(p_i - p_o) - Q_i \tag{4}$$

A single step change in production from 0 to Q at time t=0 gives the pressure changes with time in an open N-tank model

$$p(t) = p_o - \sum_{j=1}^{N} Q \frac{A_j}{L_j}(1 - \exp^{L_j t}) \tag{5}$$

and for a closed N-tank model system the following formula is used:

$$p(t) = p_0 - \sum_{j=1}^{N-1} Q \frac{A_j}{L_j}(1 - \exp^{L_j t}) - QBt \tag{6}$$

In practice the LUMPFIT program receives

1) A series of time points $t_0, t_1, \ldots, t_r, \ldots, t_s, \ldots, t_m$;
2) The production history $q_0, q_1, \ldots, q_m$, where q_i is the average production rate between the time t_{i-1} and t_i, and q_0 is the average production prior to time t_0;
3) The observed pressure or water level data which can be a much shorter series $w_0, w_r, \ldots, w_s$ at the times $t_0, t_r, \ldots, t_s$.

The calculated water level is then

$$w_{calc}(t_0) = w_0 \tag{7}$$

$$w_{calc}(t_k) = w_0 + \sum_{i=1}^{K}(q_i - q_{i-1})\left[B(t_k - t_{i-1}) + \sum_{j=1}^{N} \frac{A_j}{L_j}(1 - e^{-L_j(t_k - t_{i-1})})\right] \tag{8}$$

for k=1,...., m.

A two tank open model has N=2, and B=0. A three tank closed model has N=2 and B>0 (five coefficients). The program LUMPFIT finds the coefficients A_j, L_j and B that minimize the sum

$$Min[\sum_{l=r}^{s}(w_l - w_{calc}(t_l))^2] \tag{9}$$

where the coefficients A_j, L_j and B are complex functions of κ and σ (Axelsson, 1989).

In order to assess the quality of various fits, we define the coefficient of determination (R^2) as:

$$R^2 = \frac{\sum_{l=r}^{s} (w_l - w_a)^2 - \sum_{l=r}^{s} (w_l - w_{calc}(t_l))^2}{\sum_{l=r}^{s} (w_l - w_a)^2} \qquad (10)$$

where w_a is the mean of the observed water level data. The coefficient of determination takes values between 0 and 1, and is often written as 0-100%. It describes the fraction of the variance in the observed data about the mean, which is explained by the model.

4.2 Modelling results

Since 1982 water level has been recorded along with the production rate on a regular basis in the Hamar geothermal field. This is a very important information and the foundation for simulating and predicting the reservoir pressure changes. A lumped parameter model was created which gave an excellent comparison with the production data and the water level data. The simulation process was carried out automatically using the LUMPFIT program (Axelsson and Arason, 1992). The program was executed on a PC 486 computer. No assumptions were made a priori on the properties of the reservoir. The first step used only a closed one-tank model that represents the simplest reservoir condition. Then the model was modified and more tanks were added to the system until a satisfactory fit was achieved. The results of the last two models (Open two-tank and a closed three-tank model) are shown in Table 3. The best fitting model was a closed three-tank model, which resulted in a coefficient of determination of 99.1%. This indicates that only 0.9% of the variance in the observed water level data are not explained by this model. Figure 15 shows the comparison of the observed and calculated water level changes.

TABLE 3: Parameters of the last two lumped models

Parameter	Open-2 tank	Closed-3 tank
κ_1 (ms^2)	-90.9	87.4
κ_2	1397	1135
κ_3		48402
σ_{12} (10^{-5} ms)	33.3	40
σ_{23}	13.3	14.1
A_1	2.77036	2.84548
L_1	10.298	11.6984
A_2	0.189208	0.226293
L_2	0.233928	0.309123
B		0.0054
Coeff. of determ. (%)	98.9	99.1
R.m.s. misfit (m)	0.43	0.38

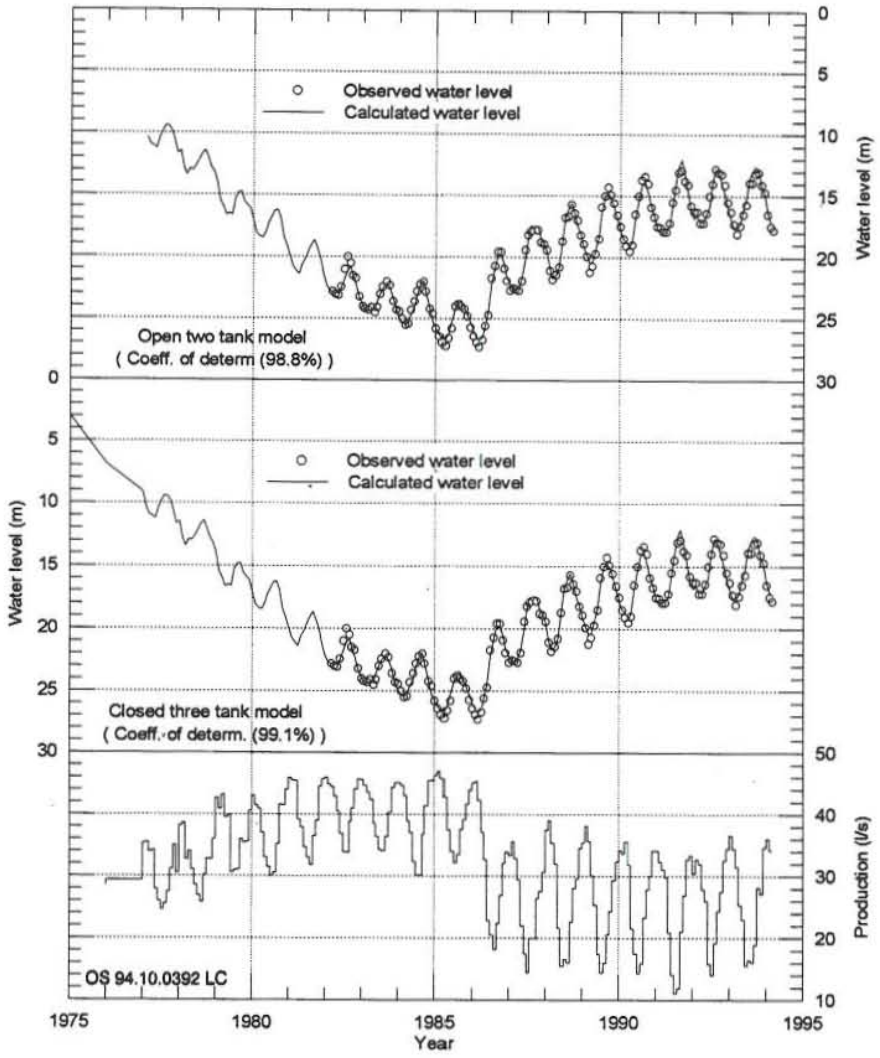

FIGURE 15: Comparison of observed and calculated water level changes

One of the main purposes of simulating a reservoir is to predict water level changes for a given future production scheme. The parameters from the best fitting lumped model are considered suitable to represent the properties of the actual reservoir. Different production rates were assumed, and future water level changes were calculated by using the best lumped parameter model. Figure 16 shows results of the predicted water level changes.

4.3 Discussion

From Figure 15, we see that the match between observed and calculated water level is quite satisfactory, in spite of the simplicity of the models. The reason for this is the diffusive nature of the pressure response of geothermal systems (Axelsson,1989).

For both the open two-tank and closed three-tank model, the coefficient of determination is very high and almost the same. This indicates that both models are suitable for the reservoir. According to the result, some conclusions can be made.

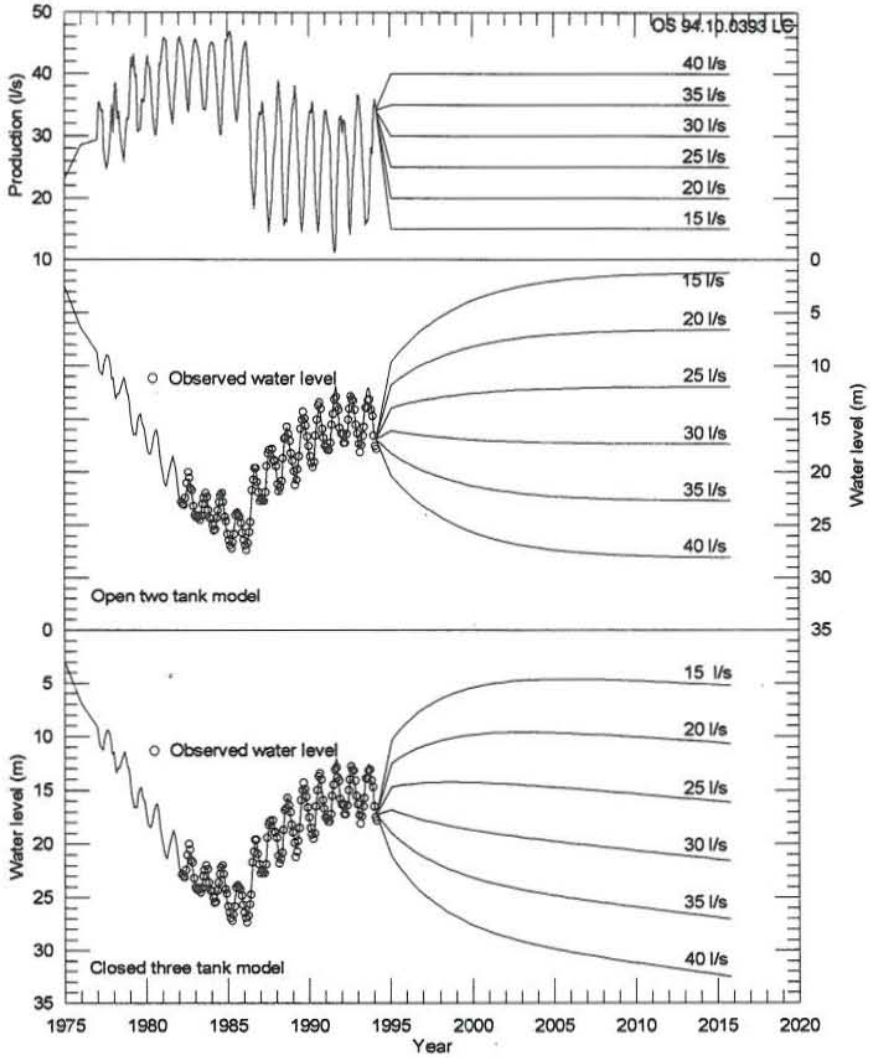

FIGURE 16: Predicted water level changes in the Hamar field

Storage. If an assumption is made that the storage, or capacitance, is controlled by the liquid and formation compressibility, the volume of the reservoir can be estimated as follows:

$$V = \frac{\kappa}{\rho_w c_t} \tag{11}$$

where ρ_w is the liquid density and c_t is the total compressibility ($c_t = \phi c_w + (1-\phi)c_r$)

From this we can estimate the volumes of the three tanks (porosity of the rock matrix is assumed 7%). The volume of tank one ($\kappa = 87.4$ ms^2) is 2 km^3, the volume of tank two ($\kappa = 1135$ ms^2) is 25 km^3, and the volume of tank three ($\kappa = 48.402$ ms^2) is 109 km^3. If the assumed aquifer thickness in the productive reservoir (tank one) is 1 km, the surface area of the reservoir is about 2 km^2.

On the other hand it can be assumed that the storage of the reservoir is controlled by the mobility of a free surface. The surface of the reservoir can then be estimated as

$$A = \frac{\kappa g}{\phi} \tag{12}$$

Calculated surfaces are, for tank one (productive reservoir) A is 12 m^2, for tank two A is 0.16×10^6 m^2, and tank three A is 6.8×10^6 m^2.

Comparing the results from the two different assumptions, the latter is more likely. Therefore, the reservoir capacitance is probably controlled by the mobility of a free surface.

Drawdown. Figure 16 shows the predictions of drawdown for different production rates. Currently the average production rate is 26 l/s with a drawdown of 15 m. The assumed production rate ranges from 15 to 40 l/s.

With 15 l/s production rate for 20 years, the water level will be at 1-5 m depending on the model. Similarly, for 40 l/s production for 20 years, the water level will be at 23-33 m below surface.

Generally, conservative predictions are obtained using closed models, and optimistic from open tank models. Therefore, keeping 15 m water level on average, it will be best to have production between 25 and 30 l/s. According to the closed three-tank model prediction, the water level will be at 22 m after 20 years of 30 l/s production.

5. ANALYSIS OF WELL TESTS

5.1 The principle of pressure transient testing

Transient pressure tests or well tests consist of recording the pressure variations versus time in a well or neighbouring wells after the flow rate from a well is changed, and subsequently, estimating the reservoir and well properties (Edwards et al., 1982). From the analysis of pressure transient tests one can deduce the permeability thickness product, kh in the drainage volume of the well, permeability, k, and condition of the well, represented by the skin factor(s).

Generally, these pressure transient testing techniques include pressure build-up, drawdown, injectivity, fall-off, and interference. For pressure transient testing analysis, several simplifying assumptions are made such as:

1) The reservoir aquifer is horizontal with constant thickness;
2) It has a uniform and homogeneous permeability;
3) It is impermeable at the top and bottom;
4) The fluid is of uniform and constant compressibility.

Although some of these assumptions may not be true, the parameter may be calculated, and can give a basis for a comparison.

These assumptions mean that the flow is radially symmetric. From the pressure diffusion equation, the conservation of mass equation can be expressed as

$$\frac{\partial p}{\partial t} = D\left(\frac{\partial^2 p}{\partial r^2} + \frac{1}{r}\frac{\partial p}{\partial r}\right) \tag{13}$$

where the diffusivity is given by

$$D = \frac{k/\nu_l}{\phi \rho_l C} \tag{14}$$

The boundary condition is

$$r \to r_w \qquad 2\pi r h \frac{k}{\nu_l} \frac{\partial p}{\partial t} = q_m \tag{15}$$

where h is the thickness of the reservoir layer and q_m is the flow rate, positive for injection and negative for production.

With the initial state condition as

$$p = p_0 \qquad for \qquad r_w \le r < \infty \tag{16}$$

this mathematical problem is difficult to solve except when r_w is assumed as 0. This is the so-called Theis solution:

$$p(r,t) - p_o = \frac{-q_m}{4\pi hk/\nu_l} Ei\ (-\frac{r^2}{4Dt}) \tag{17}$$

where Ei is the exponential integral, defined by

$$Ei(-x) = \int_x^\infty \frac{e^{-u}}{u} du \tag{18}$$

Theis solution for well test analysis. In geothermal wells, for a small x (i.e. long time) Equation 18 can be approximated as

$$Ei(x) \approx \ln(x) - \gamma \tag{19}$$

where $\gamma = 0.5772$ is Eular's constant. We now define $p^* = q_m/(4\pi kh/\nu)$ $t^* = r^2/4D$ and $p_w = p(r_w,t)$, and the exponential integral in Equation 17 becomes

$$Ei(-\frac{t^*}{t}) = 2.3\log_{10}(\frac{t}{t^*}) - 0.5772 \tag{20}$$

and Equation 17 is simplified to

$$\frac{p_0 - p_w(t)}{p^*} = 2.3\log_{10}(t/t^*) + 0.5772 \tag{21}$$

Equation 21 gives approximatly straight line when pressure changes are plotted on a semi-logarithmic scale

against time, which changes the equation to

$$p_w(t) = m \log_{10}(t) + p_{t0} \tag{22}$$

where p_{t0} is at the time t_0, and m is the slope of the asymptotic line:

$$m = \frac{2.3 q_m}{4 \pi kh/\nu_t} \tag{23}$$

By proper observation of pressure changes with time it may be possible to get a straight line using Equation 22, and calculate the two parameters, i.e. permeability thickness, kh which measures its ability to transmit fluid and storativity $c_t h$ which measures the medium's capacity to store fluid (Grant et al., 1982).

Horner method. The theoretical pressure response curve for a varying production rate can be derived by adjusting the Theis solution. If a production rate stops at a time, τ, that is the start of the build-up test. The build-up test can be considered as a special case of Equation 17

$$p_0 - p_w(t) = -p^* Ei(-t^*/t) + p^* Ei(-t^*/(t-\tau)) \tag{24}$$

In this case the logarithmic approximation of the exponential integral can be used for $\tau < t < \infty$

$$\frac{p_0 - p_w(t)}{p^*} = (2.3 \log_{10}(t/t^*) - 0.5772) - (2.3 \log_{10}((t-\tau)/t^*) - 0.5772) \tag{25}$$

The equation can be simplified by combining the logarithm terms and by writing $t = \tau + \Delta t$; where Δt is the time since shut in, or

$$\frac{p_0 - p_w(t)}{p^*} = 2.3 \log_{10}\left(\frac{\tau + \Delta t}{\Delta t}\right) \tag{26}$$

Then

$$p_w(t) = m \log_{10}\left(\frac{t + \Delta t}{\Delta t}\right) \tag{27}$$

Using semilog plot of $p_w(t)$ versus $\log_{10}[(\tau + \Delta t)/\Delta t]$ gives a straight line. This is called a Horner plot. The slope m of the straight line portion becomes the same as in Equation 23, and gives information on the permeability in the reservoir as the drawdown test.

5.2 Well tests at the Hamar reservoir

Two well tests were conducted at the Hamar reservoir in July 1988. The first was at well 10 in which the pumping test started at 16:29 July 16 and ended 13:32 on July 18, after which build-up was monitored until 9:36 July 19. Another test was taken at 13:02 July 19 until 16:05 July 23 when well 11 was producing. Water level changes were observed separately at wells 2, 4, 5, and 7. Figure 17 shows those two well tests schematically. Table 4 shows the main parameters of the well tests.

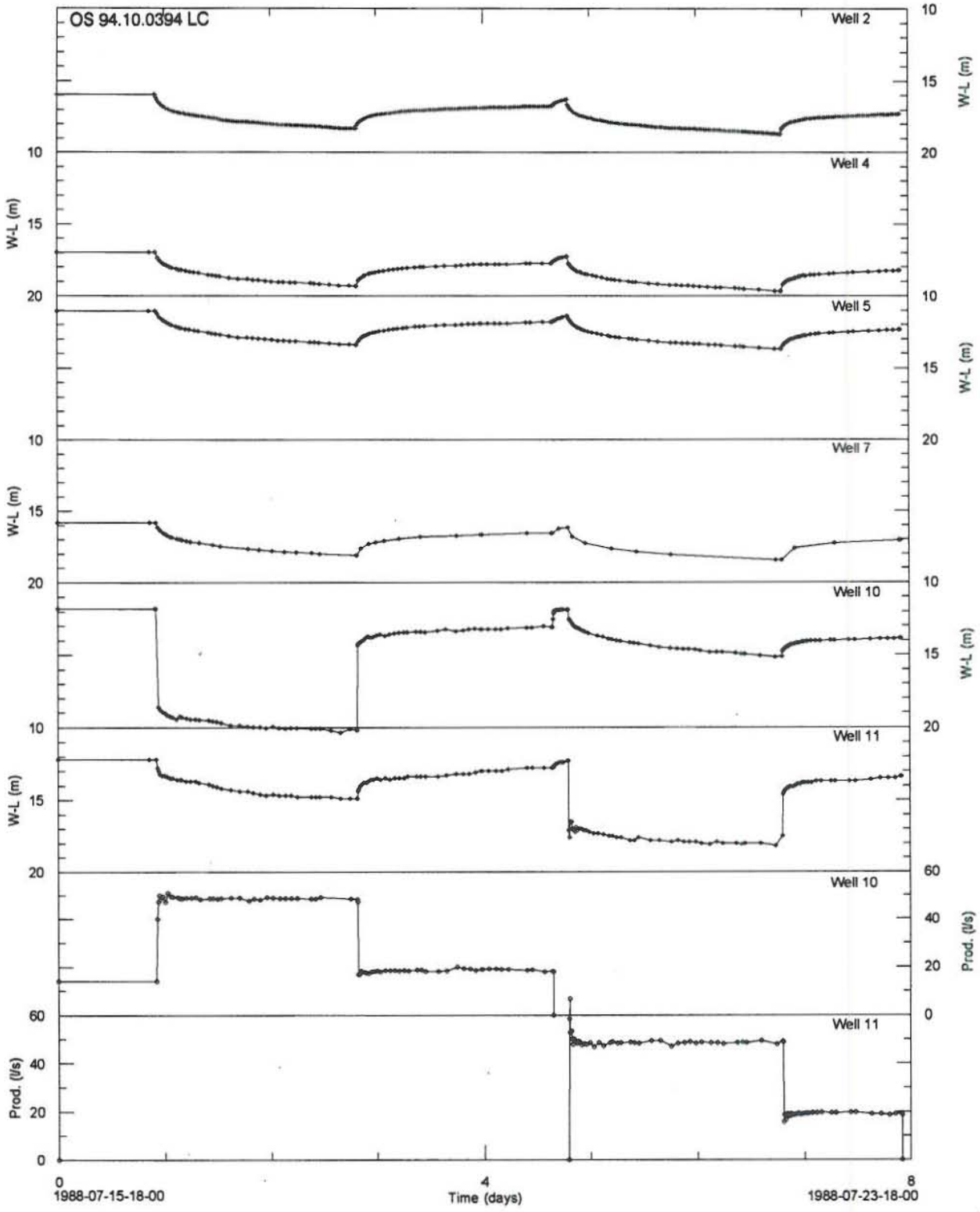

FIGURE 17: The well tests for the Hamar reservoir

On the basis of the above mentioned method, the pressure transient analysis were carried out. Figure 18 shows the asymptotic lines from Theis plots for the observation wells. The slopes m of the lines can be obtained from the plots. Figure 19 shows the Horner plots in which the slopes m can also be obtained.

TABLE 4: The main parameters of well test at the Hamar reservoir

Well no.	Initial water level (m)		Average production (l/s)		Slope - m		ν (10^{-4} m^2/s)	c (10^{-10} 1/Pa)	ϕ (%)	r* (m)
	Draw-down (m)	Build-up (m)	Draw-down (m)	Build-up (m)	Theis	Horner				
10	11.79	20.20	34.6	30.3			0.45	0.45	7	
7	15.79	18.13			1.33	0.85	0.45	0.45	7	204
5	11.05	13.38			1.38	0.93	0.45	0.45	7	203
4	16.95	19.30			1.31	0.94	0.45	0.45	7	154
2	15.96	18.83			1.29	0.88	0.45	0.45	7	155

r^* the distance between the main feedzones in the pumping well and the observation well.

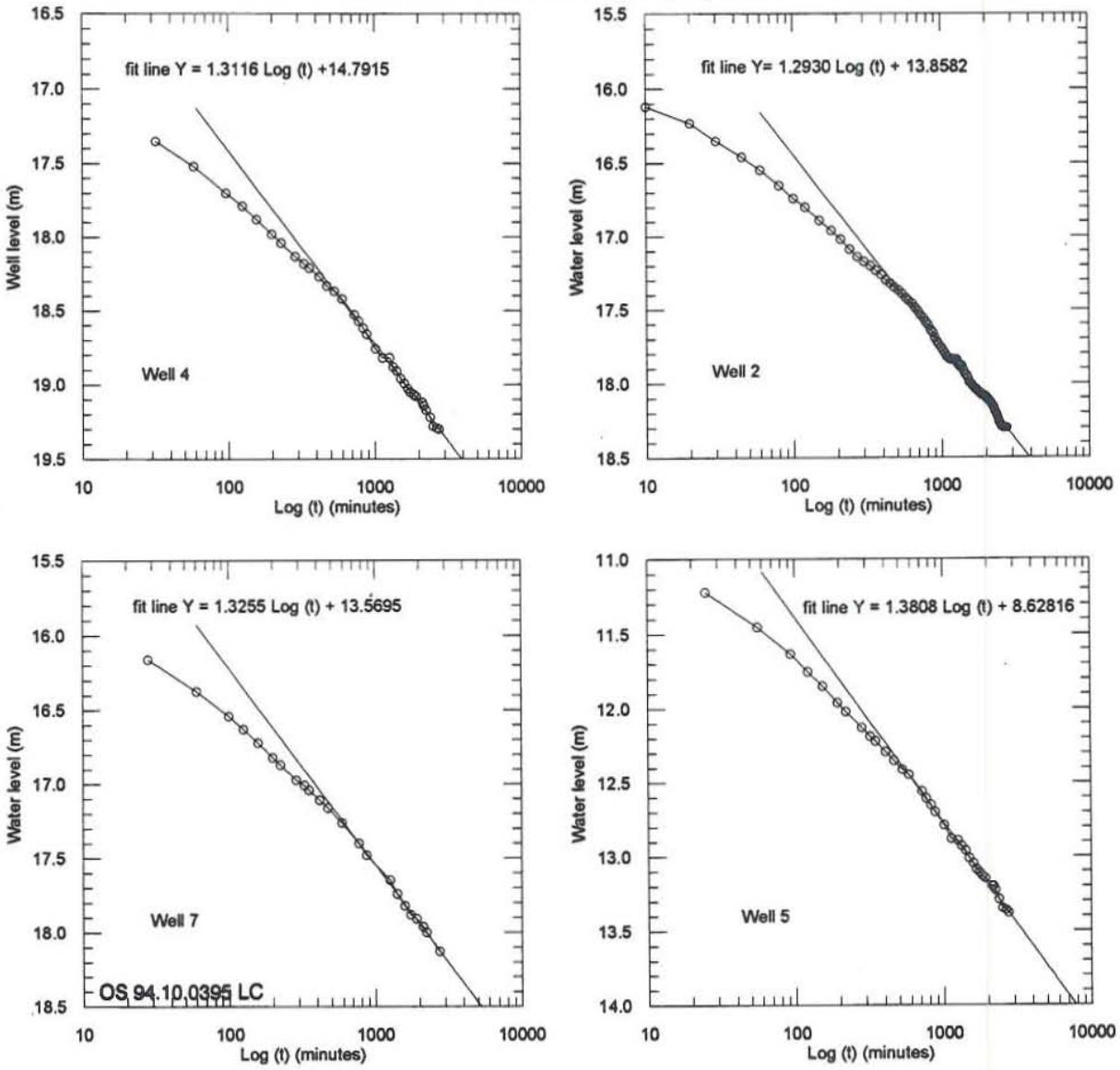

FIGURE 18: Theis plots for the pumping tests at the Hamar reservoir

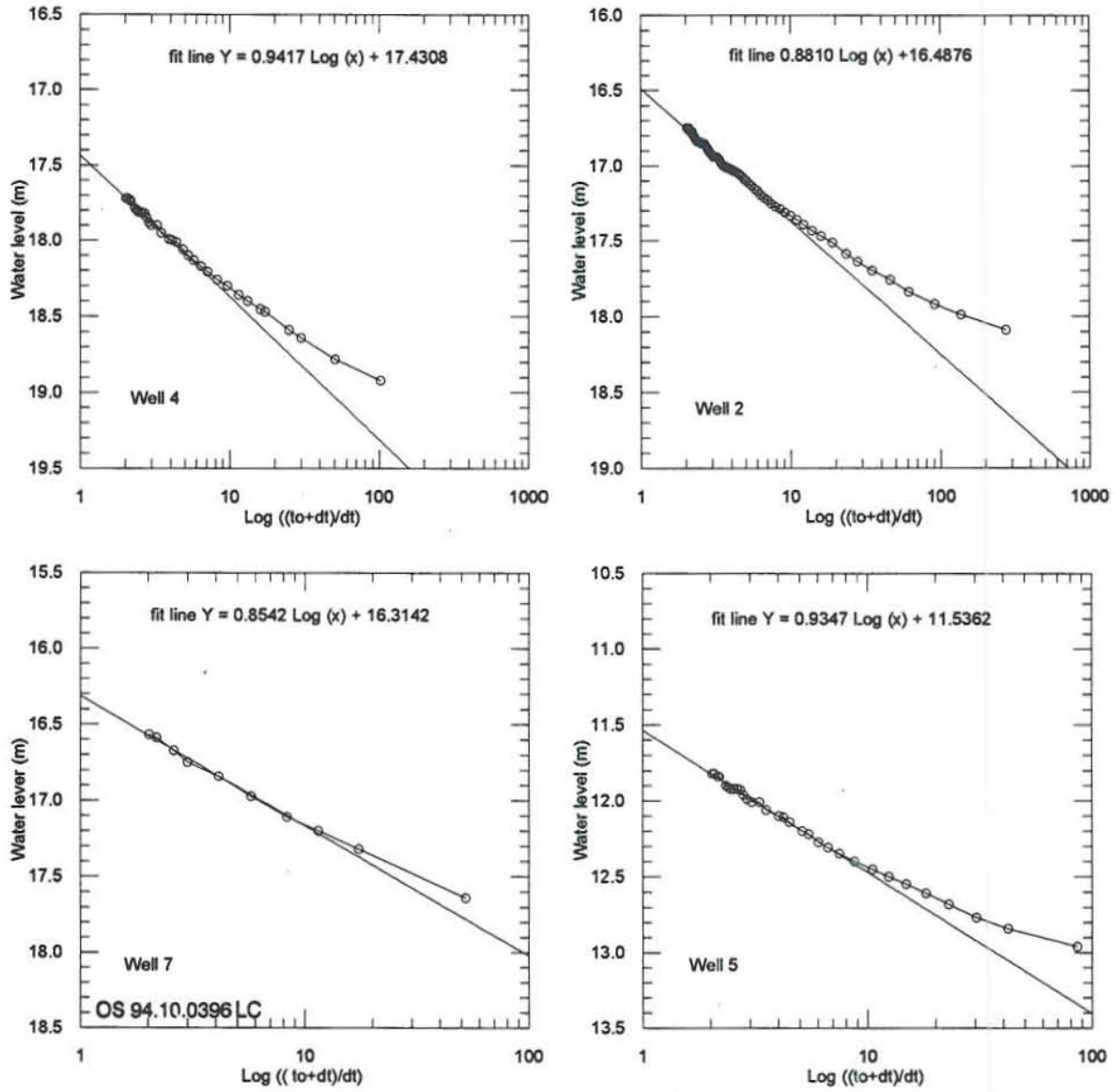

FIGURE 19: Horner plots for the build-up test at the Hamar reservoir

According to Equation 23, permeability thickness can be evaluated:

$$kh = \frac{2.3 q_m \nu}{4 \pi m} \tag{28}$$

$$c_t h = 2.25 \frac{kh}{\mu} \frac{t}{r^2} 10^{-\Delta p/m} \tag{29}$$

where Δp is the drawdown at some time t and r is the distance between the main feedzones in the pumping well and the observed wells.

Using the parameters in Table 4 and Equations 28 and 29, permeability and storativity of the reservoir can be calculated. The results are given in Table 5.

TABLE 5: The calculated results from the well tests at the Hamar reservoir

Well no.	Transmissivity kh/μ (10^{-7} m³/Pa-s)		Permeability thickness - kh (d-m)		Storativity - $c_t h$ (10^{-8} m/Pa)		Reservoir thickness - h (m)	
	Theis	Horner	Theis	Horner	Theis	Horner	Theis	Horner
7	4.77	6.54	209	286	5.4	5.4	1200	1200
5	4.60	5.98	202	246	7.5	5.8	1667	1288
4	4.84	5.98	213	246	8.8	9.5	1956	2130
2	4.92	6.31	216	277	8.8	7.3	1956	1617

5.3 Discussion

Figure 17 shows good recorded data where production rate and water level changes in production and observation wells are in accordance. The results using Theis method in the drawdown tests and Horner method in the recovery tests are similar. Comparison of the calculated permeability or storativity in different observation wells, shows that the hydrodynamic parameters are homogeneous in different directions and with depth. The aquifer thickness is in the range of 1200-2130 m. According to neutron-neutron logging data (Karlsdottir et al., 1989), it is clear that the porosity changes with depth. So the uniform permeability from different observation wells could be caused by a lot of fractures in the reservoir.

From the results of the lumped parameter model, the reservoir permeability can be calculated with the following equation (assuming it is liquid controlled):

$$\kappa = \frac{\sigma_{12} \nu \ln(r_2/r_1)}{2\pi h} \tag{30}$$

Assuming the variables for the productive reservoir to be h = 1000 m, r_1 = 25 m, r_2 = 90 m, estimated permeability by two tank model is about 3 darcies. This is bigger than that from the well test. Maybe the reason is that this result represents a bigger volume than actual or the assumptions are not suitable.

6. CONCLUSIONS

The main conclusions of this study may be summarized as follows:

1. The aquifers or feedzones in the reservoir have been identified by analysing temperature logs. The main feedzones are at 500-800 m depth.

2. The formation temperature of each well was estimated.

3. The temperature of the reservoir remains constant after most of the wells were cemented or cased in 1990.

4. The temperature distribution at various depths has been determined, and indicates that the hot water flow comes from the south.

5. The temperature cross-sections show that the high-temperature anomalies appear in areas near the dykes, that cross the field.

6. A lumped parameter model was used to simulate the reservoir. The coefficient of determination of a closed three-tank model is 99.1%. The capacity of the innermost tank, representing the wellfield area of the reservoir is about 90 ms^2. The water level changes for the next 20 years have been predicted to be less than -33 m for up to 40 l/s production.

7. Well test data analyses, using both the Theis solution and the Horner method, gave the same results. The reservoir has a transmissivity of about 5.5×10^{-7} m^3/Pa-s, coefficient of storativity of about 6.0×10^{-8} m/Pa and the reservoir thickness is about 1500 m.

ACKNOWLEDGEMENTS

I would like to express my gratitude to Dr. Ingvar B. Fridleifsson, the director of the UNU Geothermal Training Programme, for accepting me in the training programme, where I was able to participate in an excellent research environment.

I sincerely thank Ms. Helga Tulinius, my advisor, for giving me the opportunity to work under her guidance and for sharing with me many of her experiences. I am grateful for her critical review of this report. I thank Dr. Pordur Arason, also my advisor, for sharing his expertise in HP-Computers, the numerical code PT, and critical review of this report. I convey my gratitude to Dr. Gudni Axelsson, Dr. Olafur G. Flovenz, and Mr. Grimur Bjornsson for giving me many of their ideas. I wish to thank Mr. Ludvik S. Georgsson and Ms. Margret Westlund for their efficient and special guidance. I wish to express my thanks to all the lecturers, especially the staff of the reservoir engineering group, for sharing their knowledge and experience.

Finally, I dedicate this work to my wife, Hua. She is the one who made this all possible. Thanks go to my family and in-laws for their continuing support.

NOMENCLATURE

A = area of resistor (m^2)
c_w = compressibility of water (Pa^{-1})
c_r = compressibility of rock (Pa^{-1})
h = aquifer thickness
k = permeability (m^2)
L = length of resistor (m)
m = mass increase (kg)
p = absolute pressure (Pa)
Δp = pressure differential between two tanks (Pa)
q = massflow (kg s^{-1})
r = radius of reservoir
s = storativity (kg Pa^{-1} m^{-3}) for liquid-dominated reservoir, $s = \rho_w(\phi\, c_w + (1 - \phi)\, c_r)$
t = time (s)
V = volume of tank (m^3)

ϕ = porosity
κ = mass storage coefficient (capacitance) (ms^2)
ρ = density (kg/m^3)
σ = resistor (conductor) (ms), flow conductance between two tanks
ν = kinematic viscosity of geothermal water ($m^2\ s^{-1}$)
ρ_w = density of geothermal water (kg/m^3)

REFERENCES

Axelsson, G., 1989: Simulation of pressure response data from geothermal reservoir by lumped parameter model. *Proceedings of the 14th Workshop on Geothermal Reservoir Engineering, Stanford University, Ca.*, 257-263.

Axelsson, G., and Arason, P., 1992: *LUMPFIT, automated simulation of pressure changes in hydrological reservoirs. Version 3.1, user's guide.* Orkustofnun, Reykjavik, 32 pp.

Bodvarsson, G., 1982: Glaciation and geothermal processes in Iceland. *Jokull, 32,* 21-28.

Bodvarsson, G.S., Pruess, K., and Lippmann, M.J., 1986: Modelling of geothermal systems. *J. Petr. Techn., 9,* 1007-1021.

Edwards, L.M., Chilingar, G.V., Rieke, H.H., and Ferti, W.H., 1982: *Handbook of geothermal energy.* Gulf Publishing Company, 613 pp.

Flovenz, O.G., and Saemundsson, K., 1993: Heat flow and geothermal processes in Iceland. *Tectonophysics., 225,* 123-138.

Grant, M.A., Donaldson, I.G., and Bixley, P.F., 1982: *Geothermal reservoir engineering.* Academic press, 369 pp.

Karlsdottir, R., and Axelsson, G., 1986: *Production of geothermal water for Dalvik Heating Services.* Orkustofnun, Reykjavik, report OS-86044/JHD-12 (in Icelandic), 55 pp.

Karlsdottir, R., Eysteinsson, H., Smarason, O.B., Axelsson, G., and Sigurdsson, O., 1989: *Drilling of well 11 at Hamar in Svarfadardalur.* Orkustofnun, Reykjavik, report OS-89049/JHD-22B (in Icelandic), 44 pp.

Rybach, L, 1988: Determination of heat production rate. In: Haenel, R., Rybach, L., and Stegena L. (Editors), *Handbook of terrestrial heat-flow determination.* Kluwer, Dordrecht, 125-142.

Saemundsson, K., 1970: *Report on geothermal investigations at Dalvik in August 1970.* Orkustofnun, Reykjavik, report (in Icelandic), 16 pp.